Biol Cybern (2008) 99:105–114
DOI 10.1007/s00422-008-0246-9

ORIGINAL PAPER

Biological Cybernetics

Complex evolution of spike patterns during burst propagation through feed-forward networks

Jun-nosuke Teramae · Tomoki Fukai

Received: 26 December 2007 / Accepted: 3 June 2008 / Published online: 7 August 2008

Abstract Stable signal transmission is crucial for information processing by the brain. Synfire-chains, defined as feed-forward networks of spiking neurons, are a well-studied class of circuit structure that can propagate a packet of single spikes while maintaining a fixed packet profile. Here, we studied the stable propagation of spike bursts, rather than single spike activities, in a feed-forward network of a general class of excitable bursting neurons. In contrast to single spikes, bursts can propagate stably without converging to any fixed profiles. Spike timings of bursts continue to change cyclically or irregularly during propagation depending on intrinsic properties of the neurons and the coupling strength of the network. To find the conditions under which bursts lose fixed profiles, we propose an analysis based on timing shifts of burst spikes similar to the phase response analysis of limit-cycle oscillators.

1 Introduction

Cortical neurons often exhibit spike sequences that have millisecond precision (Prut et al. 1998). This observation suggests that cortical circuits contain feed-forward networks, or synfire chains. Dynamics of spike propagation throughout the networks have been extensively studied under various conditions (Abeles 1991; Diesmann et al. 1999; Cateau and Fukai 2001; Teramae and Fukai 2007a,b). Recent experiments have shown that neurons in the high vocal center of songbirds exhibit sequences of bursts of several spikes while singing (Hahnloser et al. 2002). Individual neurons generated bursts at precise times during a motif of the song, possibly providing a precise temporal representation within the song. These results indicate that the neural circuit of the songbird may have a feed-forward network structure that propagates bursts rather than single spikes (Jin et al. 2007).

Bursting can be found in a variety of physical and biological systems (Rinzel and Troy 1982; Elezgaray and Arneodo 1992; Meucci et al. 2002). In the brain, bursting may arise from several different mechanisms, including intrinsic properties of isolated neurons and population dynamics of neurons (Terman 1991; Nowotny and Rabinovich 2007). For example, in spatially extended systems, intrinsic or external randomness of the system can evoke propagation of intermittent activities, which result in bursting (Chaté and Manneville 1987; Osipov et al. 2005). Cortical 'up' states may be an example of such a population activity in which bursts of spikes propagate through recurrent neuronal networks (MacLean et al. 2005). Although the functional role of 'up' states remains elusive, the propagating bursts may be involved in faithful signal processing in the brain.

Here, we use the term 'bursting' in a more limited sense to refer to the spike sequences generated by intrinsic and deterministic dynamics of single neurons. This type of bursting appears when slowly evolving variables modify the limit-cycle oscillation of fast variables (Rinzel 1987; Izhikevich 2000). In neuronal firing, the membrane potential and spike generating channels serve as fast variables, while the dynamics of calcium or slow ionic channels are the slow variables. These slow variables operate as bifurcation parameters that can turn bursting off by driving the fast subsystem into a state where only a mono-stable fixed point exists. The interactions between the two sets of variables with different time

J. Teramae (✉) · T. Fukai
Laboratory for Neural Circuit Theory,
RIKEN Brain Science Institute, Hirosawa 2-1,
Wako, Saitama 351-0198, Japan
e-mail: teramae@brain.riken.jp; teramae@riken.jp

T. Fukai
e-mail: tfukai@brain.riken.jp

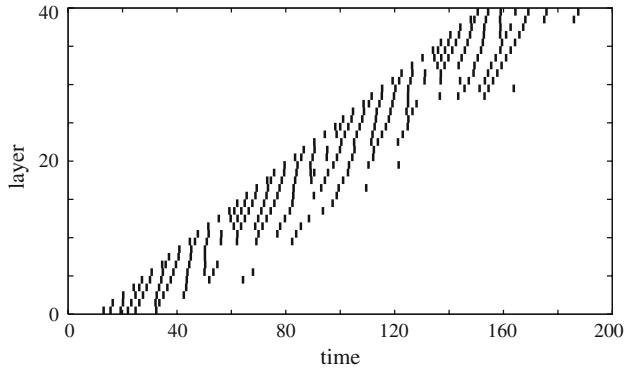

Fig. 1 Propagation of bursts with complex evolution of profiles through a feed-forward network, calculated numerically from Eq. 7. Each layer of the feed-forward network has only one neuron. *Short vertical bars* indicate the spike timings of these bursting neurons

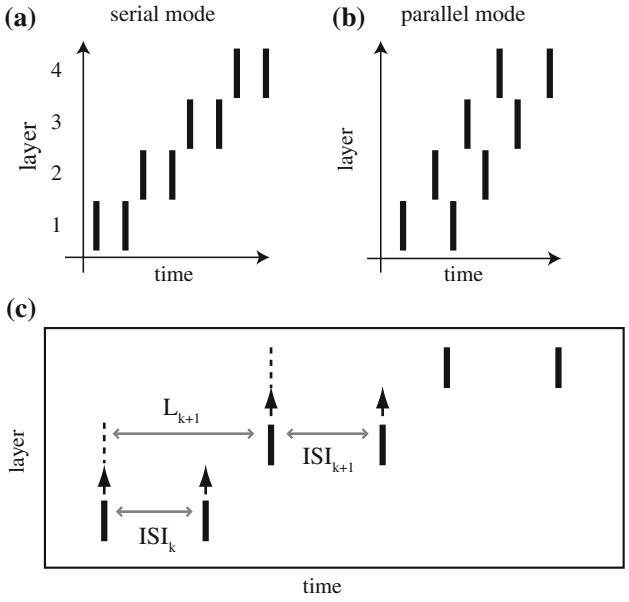

Fig. 2 Propagation of doublet spikes. **a** "Serial-mode" doublet propagation. The second spike of the kth layer precedes the first spike of the $(k+1)$th layer. **b** "Parallel-mode" doublet propagation. The second spike in the kth layer follows the first spike in the $(k+1)$th layer. **c** Relationships between output spike timings and intervals of input spikes determine the evolution of the doublet profile through layers

scales create a rich variety of phenomena (Wang 1993; Han et al. 1995; Raghavachari and Glazier 1999; Rulkov 2001; Ivanchenko et al. 2004; Shilnikov and Cymbalyuk 2005; Belykh et al. 2005; Medvedev 2006; Takekawa et al. 2007).

In this paper, we examine spike propagation inherent in bursting dynamics, that is, stable burst propagation through a feed-forward network without a fixed burst profile (Fig. 1). We find that bursts can propagate stably showing complex temporal profiles, a quality that is absent from propagation of single spikes. Spatio-temporal patterns of complex propagation may broaden possible signal transmissions in networks of neurons. To study propagation with a continually evolving spike pattern, we analytically calculate the shift of spike timing induced by perturbing inputs during a burst. From this, we derive a recursive relationship for the timing of output spikes in adjacent layers of a feed-forward network. The method is similar to the phase response analysis of limit-cycle oscillators (Kuramoto 1984). This recursive relationship allows us to clarify the conditions for burst propagation without a fixed profile and to study the evolution of spike patterns during burst propagation. We apply the method to an important class of excitable bursting neurons (Rinzel 1987; Izhikevich 2000; Guckenheimer and Holmes 1983). In addition, we show numerically that burst propagation with complex evolving profiles is robust against background noise.

2 Propagation velocities of doublet spikes

To illustrate the essence of burst propagation, we first consider the propagation of doublet spikes through a feed-forward network in which each layer has only one excitable bursting neuron. We say that neurons are 'excitable bursting' when they have a stable resting potential and respond to an impulse input with at least two spikes. The spike timing of a doublet burst is characterized by the latency of the first spike, L, and the inter-spike interval, ISI, between the first and second spikes (Fig. 2). The latency is measured from the arrival of the first input from the previous layer. We denote their intrinsic values for a pulse stimulus as L^0 and ISI^0 (Fig 3a), which generally differ from L and ISI obtained in networks since following spikes from the previous layer perturb the spike timing. For the time being, we ignore the effect of noise and assume that synaptic input is represented by an instantaneous pulse given by a delta-function with constant coupling strength, ε. Later we will discuss those cases where a burst consists of more than two spikes, where each cell layer has more than one neuron and where the individual neurons receive noisy input.

As illustrated in Fig. 2, two different modes of doublet propagation seem to be possible depending on the timing of the second spike. When the latency L of the first spike is larger than the ISI, the second spike of a burst in the previous layer arrives before the first spike of the burst in the current layer. We call this type of propagation "serial-mode" propagation (Fig. 2a). In contrast, when L is shorter than the ISI, the second input arrives after the first spike, and the burst propagation is called "parallel mode" (Fig. 2b). In these figures, the first and the second spikes of a burst are shown as if they are propagating with the same velocity. However, they have, in general, different velocities. In the next section, we will derive the criteria for the generation of these two modes and prove that, in parallel-mode propagation,

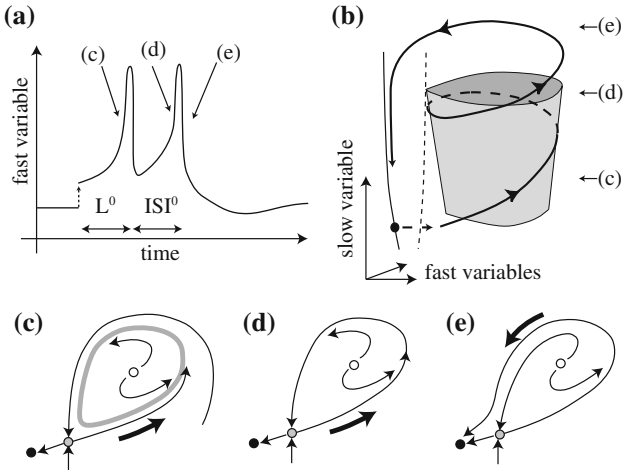

Fig. 3 Intrinsic properties of an excitable bursting neuron which appears via a homoclinic bifurcation. **a** Response of the bursting neuron to an impulse input (*dotted arrow*). Trajectory of the bursting neuron (*thick black arrows*) in a three-dimensional phase space (**b**) and in two-dimensional slices perpendicular to the slow variable (**c**–**e**). Thin line in (**b**) and *black circles* in (**c**–**e**) are stable fixed points, dotted line in (**b**) and *small gray circles* in (**c**–**e**) are saddle points, *gray surface* in (**b**) and the *thick gray circle* in (**c**) are limit cycles, and *open circles* in (**c**–**e**) are unstable fixed points. *Arrows* from the saddle are unstable manifolds and *arrows* into the saddle are stable manifolds. The limit cycle (**c**) grows until it collides with the saddle and its stable and unstable manifolds at the homoclinic bifurcation point (**d**) and then disappears (**e**)

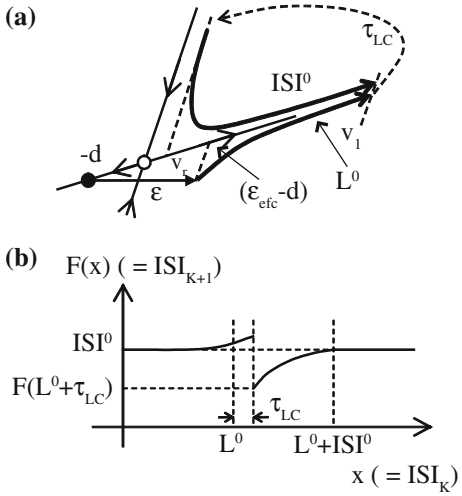

Fig. 4 **a** Dynamics of the fast subsystem in the vicinity of the saddle point. *Dotted straight lines* indicate projections to the unstable direction along the stable direction. **b** ISI_{k+1} as a function of ISI_k

the second spike always propagates faster than the first one. Therefore, parallel-mode propagation never occurs with a fixed burst profile as in Fig. 2b. The second spike of this mode chases the first one until the second eventually catches up with the first. These spikes, then, restart chasing from an initial interval and this endless chasing is the origin of the continual evolution of burst profiles. Actually, we can see a similar chase in Fig. 1 where the second and later spikes propagate faster than the first spike until they catch up with the first one.

3 Theoretical analyses of propagation

3.1 Recursive relationship of ISI between adjacent layers

The difference between the propagation velocities of the first and second spikes is characterized by the evolution of ISI between them. Their velocities are the same if the ISI is kept constant while a burst travels through the layers, whereas the second spike propagates faster (or slower) than the first one if the ISI decreases (or increases) with propagation through layers. In a feed-forward network, the ISI at a layer is given as a function of the interval between two input spikes. Since the ISI of the kth layer is the interval of input to the $(k+1)$th layer, the recursive relationship, $\mathrm{ISI}_{k+1} = F(\mathrm{ISI}_k)$, describes the evolution of spike timing along the layers. Since synaptic couplings are instantaneous pulses, the function $F(\mathrm{ISI}_k)$ is independent of ISI_k when $\mathrm{ISI}_k < L^0$ and $\mathrm{ISI}_k > L^0 + \mathrm{ISI}^0$ (see Fig. 4b for example). ISI is kept constant across layers only when the function F has a stable fixed point ISI_s satisfying $\mathrm{ISI}_s = F(\mathrm{ISI}_s)$ and $\left|F'(\mathrm{ISI}_s)\right| < 1$, where the dash denotes the derivative with respect to ISI. A stable solution to ISI_s always exists in the serial-mode propagation since $F(\mathrm{ISI}_k)$ is constant and independent of ISI_k when $\mathrm{ISI}_k < L^0$. In contrast, as we will see later, in almost all ranges of parameter values, a stable solution to ISI_s does not exist in parallel-mode propagation. Interestingly, this absence of ISI_s does not mean the failure of doublet spike propagation. Rather, it implies a novel form of stable burst propagation with a non-converging burst profile.

3.2 Excitable bursting appears via homoclinic bifurcation

An analytical evaluation of the function F is possible when bursting appears via homoclinic bifurcation (Fig. 3), where the limit cycle passes through the neighborhood of the saddle. This bursting is the most common type of excitable bursting and is commonly observed in the bursting of the Hindmarsh-Rose model (Hindmarsh and Rose 1984) and many realistic neuron models (Chay and Keizer 1983; Butera et al. 1999; Vries and Sherman 2000; Izhikevich 2006). Before burst emission, the fast subsystem of this type of bursting neuron is in a bistable state that consists of a stable fixed point and a limit cycle separated by a saddle point (Fig. 3c). A strong enough spike input pushes the fast variables from the fixed point to the basin of attraction of the limit-cycle oscillator beyond the stable manifold of the saddle. This initiates a rotation along the limit cycle and a series of spikes, which in

turn move the slow variables to modify the fast phase space until the limit cycle is annihilated by a homoclinic bifurcation or a collision with the saddle point. This annihilation terminates the series of spikes and results in bursting. We can assume that the limit cycle passes through the neighborhood of the saddle point. Since the dynamics are slow near the saddle, the fast variables stay long in the neighborhood, while they travel the remaining part of the limit cycle in a relatively short time denoted by τ_{LC}. We can also assume that the values of the slow variables do not change while the fast variables pass through the vicinity of the saddle. The function F is, therefore, derived only from the fast dynamics in the neighborhood of the saddle with fixed values of the slow variables.

The system's time evolution near the saddle is described by a linear summation of stable and unstable dynamics (Fig. 4a). Projecting the fast variables to the unstable direction along the stable one gives a reduced one-dimensional equation of the unstable mode u,

$$\dot{u} = \frac{\lambda}{d} u(u + d), \tag{1}$$

where λ (> 0) is the unstable eigenvalue of the saddle and d is the position of the stable fixed point measured along the unstable direction. The two parameters take different values before (λ_1 and d_1) and after (λ_2 and d_2) the first spike, since the slow variables may increase during the spike generation. Setting spike threshold to $u_1 (>> \mathrm{d})$ and integrating Eq. 1 gives the timing of spikes as

$$t_s(u_0; \lambda, d) = \frac{1}{\lambda} \log \left(\frac{u_1(u_0 + d)}{u_0(u_1 + d)} \right), \tag{2}$$

under initial condition $u(0) = u_0$. Using t_s, the intrinsic times of the first and second spikes are determined by,

$$L^0 = t_s(\varepsilon_u - d_1; \lambda_1, d_1) \tag{3}$$

and

$$\mathrm{ISI}^0 = t_s(u_r; \lambda_2, d_2) + \tau_{\mathrm{LC}}, \tag{4}$$

where ε_{u} is the input strength measured along the unstable direction and u_{r} is the effective initial value of u after the first spike, which is almost equal to, but slightly smaller than, the distance of the limit cycle from the stable direction of the saddle along the u-axis. If the attraction of the limit cycle is infinitely strong, the two values should be exactly the same. The dimension of ε is equal to dimensions of u and d. Then, $F(x)$ is given as,

$$F(x) = \begin{cases} \mathrm{ISI}^0, x < L^0, L^0 + \mathrm{ISI}^0 < x \\ x - L^0 - \tau_{\mathrm{LC}} + \max\left(t_s\left(u\left(x - L^0 - \tau_{\mathrm{LC}}, v_r\right)\right.\right. \\ \quad \left.\left. + \varepsilon; \lambda_2, d_2\right), 0\right), L^0 < x < L^0 + \mathrm{ISI}^0 \end{cases} \tag{5}$$

where $u(t, u_0)$ is the solution to Eq. 1 with $\lambda = \lambda_2$ and $d = d_2$ for initial value u_0. Taking the maximum in Eq. 5 is necessary to ensure causality. Fig. 4b displays a typical profile of F. The function $F(x)$ is generally discontinuous at $x = L^0$. When the dynamical state passes the interval $L^0 < x < L^0 + \tau_{\mathrm{LC}}$ or approaches the point $x = L^0$, $F(x)$ becomes slightly larger than ISI^0 since the burst input kicks the fast variables out of the limit-cycle trajectory. We do not take this small effect into account in the present analysis. Since the function t_{s} is sensitive to external input when the fast variables stay near the stable manifold of the saddle, the value of $F(x)$ is suddenly decreased when x goes beyond L^0. Serial-mode propagation occurs when $L^0 - \mathrm{ISI}^0 > 0$ (see Fig. 6a and c for example). Solving this inequality, we find that the weak coupling regime, $\varepsilon < \varepsilon_{\mathrm{c}}$, always shows serial-mode propagation since L^0 is a monotonically decreasing function of ε while ISI^0 is independent of ε. The critical value ε_{c} is the unique solution to $L^0 = \mathrm{ISI}^0$.

When $\varepsilon > \varepsilon_{\mathrm{c}}$, doublet propagation occurs in parallel mode without a fixed profile if the equation $x = F(x)$ does not have stable solutions in the range $L^0 + \tau_{\mathrm{LC}} < \tau < L^0 + \mathrm{ISI}^0$. However, the propagation itself can be stable. Since $u(t, u_0)$ is an increasing function of t, $t_s(u_0, \lambda, d)$ is a decreasing function of u_0, and the slope of F is always smaller than 1,

$$\frac{\mathrm{d}F}{\mathrm{d}x} = 1 + \frac{\mathrm{d}t_s}{\mathrm{d}u} \left. \frac{\partial u}{\partial t} \right|_{t=x} \leq 1. \tag{6}$$

Taking into account the right boundary condition, $F(L^0 + \mathrm{ISI}^0) = \mathrm{ISI}^0 < L^0 + \mathrm{ISI}^0$, we obtain the condition that ensures parallel-mode propagation with a fixed profile as, $F(L^0 + \tau_{\mathrm{LC}}) > L^0 + \tau_{\mathrm{LC}}$, that is, $t_{\mathrm{s}}(\varepsilon_{\mathrm{u}} + u_{\mathrm{r}}, \lambda_2, d_2) > t_{\mathrm{s}}(\varepsilon_{\mathrm{u}} - d_1, \lambda_1, d_1)$. However, since the initial state u_{r} always satisfies $\varepsilon_{\mathrm{u}} + u_{\mathrm{r}} > \varepsilon_{\mathrm{u}} - d_1$, the condition cannot be satisfied if $\eta_2 = \lambda_2/d_2 \geq \eta_1 = \lambda_1/d_1$. Even when $\eta_2 < \eta_1$, the condition is satisfied only by values of ε greater than ε_m, where ε_m is the solution to $t_{\mathrm{s}}(\varepsilon_m + u_{\mathrm{r}}, \lambda_2, d_2) = t_{\mathrm{s}}(\varepsilon_m - d_1, \lambda_1, d_1)$. Since $\varepsilon_m \sim |\eta_2/\eta_1 - 1|^{-1}$, the value of ε_m increases rapidly as the difference $\eta_1 - \eta_2$ becomes small, and the input strength can easily exceed the acceptable value determined by $u_0 + \varepsilon_u < u_1$. Thus, we can conclude that, except in the extreme case where $d_2/d_1 >> \lambda_2/\lambda_1$ and ε is also extremely large, propagation in the parallel-mode occurs only with a continually evolving profile, but not with a fixed burst profile.

The above analysis using the function F revealed why the burst profile can continue to change during its propagation. In parallel-mode propagation, the second spike of the k-th layer arrives after the first spike of the $(k + 1)$th layer and advances the timing of the second spike of the $(k+1)$th layer since $F(x) < x$ for $L^0 + \tau_{\mathrm{LC}} < \tau < L^0 + \mathrm{ISI}^0$ (see Fig. 6d). Thus, the second spike propagates faster than the first spike until it finally catches up with the first one. The spikes repeat this endless chase, generating a continually evolving burst profile.

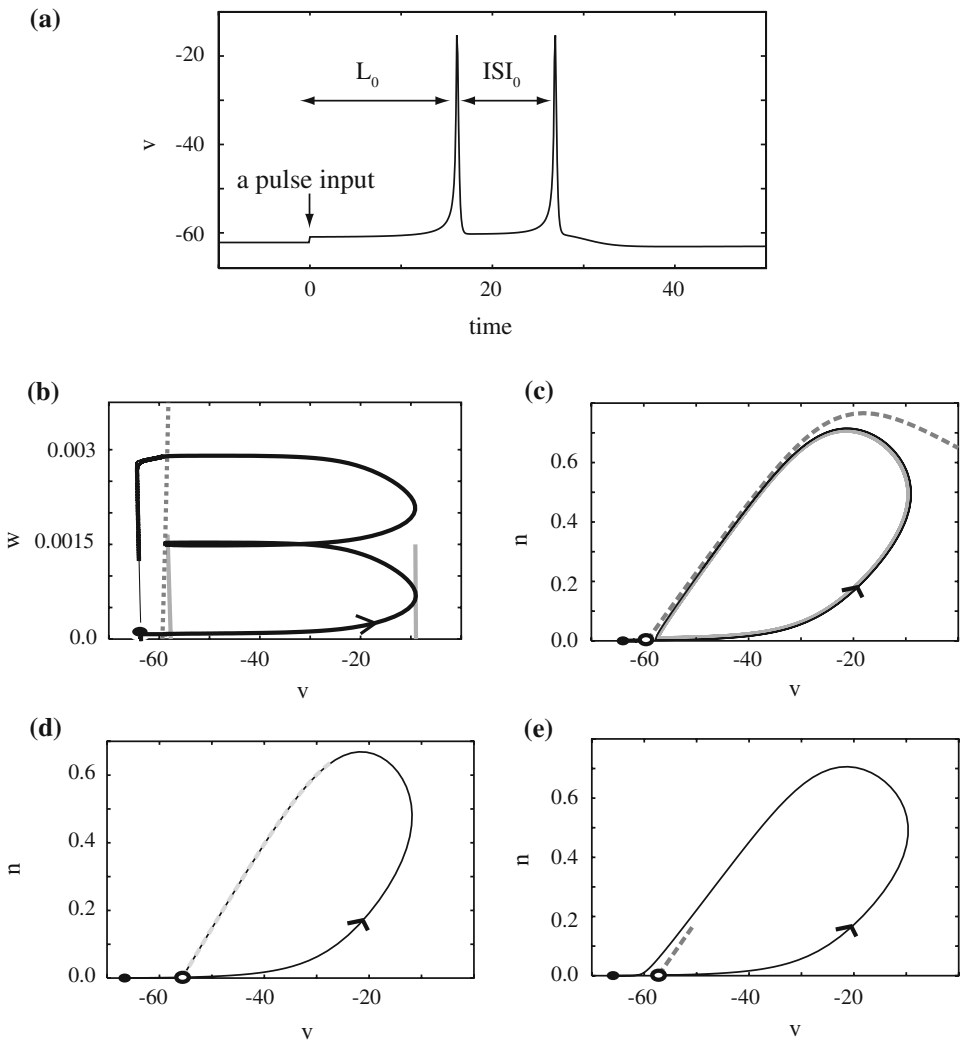

Fig. 5 Single cell properties of the model neuron calculated numerically from Eq. 7. **a** The membrane potential v responds by a burst to a pulse input. **b** Bifurcation diagram in v–w plane and the trajectory (*thick black line*) of the bursting elements. *Thin black line*, *gray dotted line* and *gray solid line* are the stable fixed point, the saddle point and the limit cycle of the fast two-dimensional subsystem, respectively. *Filled circle* is the stable fixed point of the whole three-dimensional system. **b**–**d** Phase diagram of the fast subsystem before (**b**), near (**c**) and after (**d**) homoclinic bifurcation. *Thick black curves* are unstable manifolds and *gray dotted curves* are stable manifolds of the saddles shown as *open circles*. *Filled circles* are stable fixed points. *Thick gray line* in (**b**) is the limit cycle

The function $F(x)$ can be related to the phase response curve (PRC, $Z(\theta)$) of limit-cycle oscillators. PRC is defined as the phase shift induced by an infinitesimal perturbation along the oscillatory orbit (Kuramoto 1984). During a burst, the evolution of slow variables continuously modulates the limit cycle consisting of the fast subsystem. The limit cycle is, however, sufficiently stable for defining a PRC if the modulations remain small. Mathematically, the phase shift coincides with PRC when the shift is measured with a post-stimulus period which asymptotically relaxes back onto the limit cycle from the perturbed state. Practically, however, the timing shift of next spike induced by an input is well approximated by PRC (Hansel et al. 1995; Netoff et al. 2005). This approximation gives the relationship between $F(x)$ and PRC as $Z(\theta)\varepsilon = 2\pi\left(1 - F\left(\tau\left(\theta\right)\right)/T_{20}\right)$, where $\tau\left(\theta\right) = L_0 + \left(\mathrm{ISI}_0/2\pi\right)\theta$. As PRCs have been measured in real neurons (Reyes and Fetz 1993; Galan et al. 2005; Tsubo et al. 2007a,b), similar experiments enable us to record $F(x)$ directly from real bursting neurons.

4 Numerical simulations of the neuron chain

To confirm the above results, we calculate burst propagation numerically using a continuous differential equation for a model of an excitable bursting neuron (Izhikevich 2006):

$$\begin{cases} \dot{v} = -I_{\mathrm{Na}} - I_K\left(n\right) - I_M\left(w\right) - I_{\mathrm{leak}} \\ \qquad +\varepsilon \sum_{\mathrm{pre}} \sum_{\mathrm{spike}} \delta\left(t - t_{\mathrm{pre,spike}}\right) \\ \tau_n \dot{n} = n_\infty\left(v\right) - n \\ \tau_w \dot{w} = w_\infty\left(v\right) - w, \end{cases} \tag{7}$$

where $t_{\mathrm{pre,spike}}$ are the times of input spikes from the previous layer. Fast variables are membrane potential v and gating variable n of a fast spike-generating channel, while gating variable w works as a slow variable. The mathematical details of the ionic channels are described in the Method section. Figure 5 summarizes the intrinsic properties of the model neuron. Comparing these figures to Fig. 3, we can see that the model exhibits a homoclinic bursting. We arrange

the model neurons in a feed-forward chain in which each layer has a single neuron. The coupling between adjacent layers is a delta-function applied to v with strength ε. When the coupling strength is small, but is large enough to initiate spikes in the next layer, bursts propagate through serial modes (Fig. 6a). The fixed point on the function F, i.e., ISI_s denoted by the square symbol in Fig. 6c, is equal to ISI^0. Bursts propagate while maintaining a fixed profile. In contrast, when ε is strong, the burst propagation turns into parallel mode (Fig. 6b). The function $F(\mathrm{ISI})$ has no fixed points and the value of ISI_k changes throughout propagation. The analytically derived function F accurately predicts these changes in ISI (Fig 6d). As indicated by the form of $F(x)$, the value of x falls in a range of $x < L^0$ and returns to $F(x) = \mathrm{ISI}^0$ in its evolution. Therefore, the evolution of burst profile during doublet parallel-mode propagation is always periodic. In the specific examples shown in Fig. 6b and d, the period is three. As mentioned in the previous section, if η_1 is much larger than η_2 and if ε is sufficiently large, even parallel-mode propagation may exceptionally display a fixed temporal profile. However, we could not find such a set of parameter values in the present simulations. Figure 7a shows a phase diagram that summarizes the burst propagation in this model. As we expected, the burst propagation displays a fixed profile only in small regions of parameter values for relatively weak coupling strength ε Fig. 7b). The

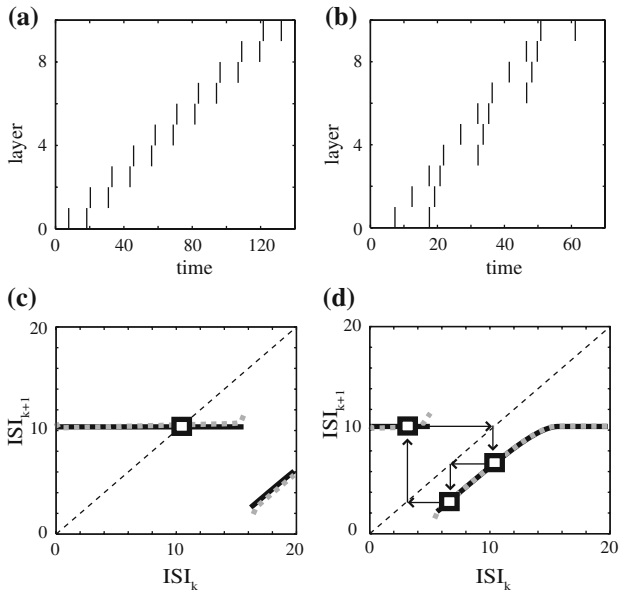

Fig. 6 **a** Propagation of doublet spikes calculated numerically from Eq. 7 with $g_M = 6.2$ and $\varepsilon = 1.25(< \varepsilon_c)$. Other parameters are the same as in Fig. 1. **b** Similar plot of (**a**) but for a larger coupling strength, $\varepsilon = 1.7(> \varepsilon_c)$. **c**, **d** The function $F(\mathrm{ISI}_k)$ calculated numerically, gray dotted curves, from the single neuron models corresponding to (**a**) and (**b**), respectively. *Black curves* are analytical results. *Open squares and connecting arrows* are derived from (**a**) and (**b**) to show the evolution of the doublet profile along the layers

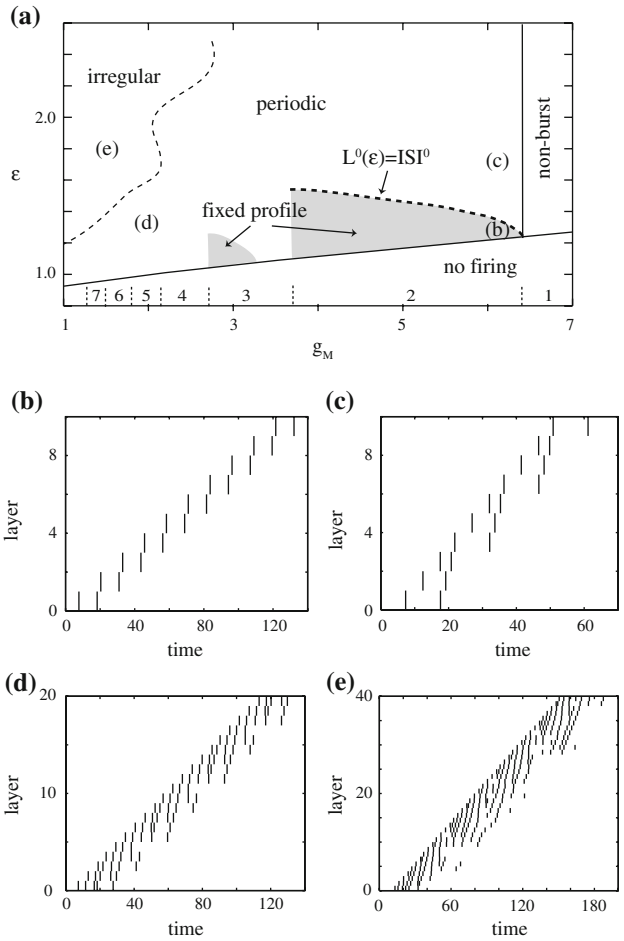

Fig. 7 Phase diagram and raster plots of burst propagation. **a** The integers above the abscissa indicate the number of spikes generated by a single neuron in response to a pulse input (see Fig. 5a). *Parenthetic alphabets* show the parameter values used below in raster plots. *Thick dotted line* is the boundary between the two propagation modes predicted by our theoretical analysis. Burst propagation shows (**b**) a fixed [corresponding to the *shaded area* in (**a**)], **c**, **d** a cyclic or **e** an irregularly changing temporal profile. We classify the bursting profile as "irregular" when we cannot detect any periodicity after propagation over 100. layers

border between doublet propagation with and without fixed profiles is well fitted by the theoretical curve. Burst propagation exhibits more complex evolving patterns when it consists of more than two spikes (Fig. 7c, d). Similar to doublet propagation, the endless chase among spikes is the cause of continuing evolution of the burst profile. However, the analysis with a recursive map similar to $F(x)$ is complicated when a burst contains more than two spikes, since the phase space of the recursive relationship would be multi-dimensional and the number of intraburst spikes may change from layer to layer. We show an example of propagation with an irregularly changing profile in Fig. 7e. Unlike doublet propagation, burst propagation looks chaotic rather than periodic, although

whether this propagation is really chaotic should be clarified by future studies.

5 Burst propagation under a noisy environment

5.1 Chain of single neurons

So far, we have neglected the effects of background noise on burst propagation. Background noise may disturb faithful signal propagation (Destexhe and Contreras 2006; Van Rossum et al. 2002; Mehring et al. 2003; Fellous et al. 2004; Beggs and Plenz 2004) and, moreover, may create nontrivial effects in nonlinear systems (Gammaitoni et al. 1998; Zhou and Kurths 2002; Teramae and Tanaka 2004, 2006). To examine the robustness of the present burst propagation against background noise, and to examine the effect of noise on the complex evolution of the profile of bursts, we conduct numerical simulations of burst propagation in the presence of noise. We first treat the case where each cell layer consists of a single neuron, as in the previous sections. Figure 8a is a phase diagram which summarizes the success and failure of burst propagation at various values of noise intensity σ and coupling constant ε. The region of failure can be further divided into three parts. If both σ and ε are small, a presynaptic input often fails to activate a postsynaptic neuron, and the propagation stops midstream (Fig. 8b). When σ is sufficiently large, the noise may activate any neuron in any layer, randomly starting burst propagation (Fig. 8c). The boundary between the two phases is ambiguous since both accidental stop and start can occur near the boundary. When σ is small but ε is sufficiently large, the last spikes in individual bursts are delayed and propagate as separate single spikes (Fig. 8d). When the last spikes are generated, the cells are in a period of after-hyperpolarization induced by the preceding burst of spikes. Therefore, the latency of spike generation is prolonged and input from the previous layer can evoke only single spikes rather than bursts. In a mid-range of ε, bursts propagate successfully as long as σ is sufficiently small (Fig. 8e). The critical value of ε necessary to overcome the disturbance of noise often exceeds the boundary between serial and parallel-mode propagation. Therefore, stable burst propagation shows an evolving temporal profile.

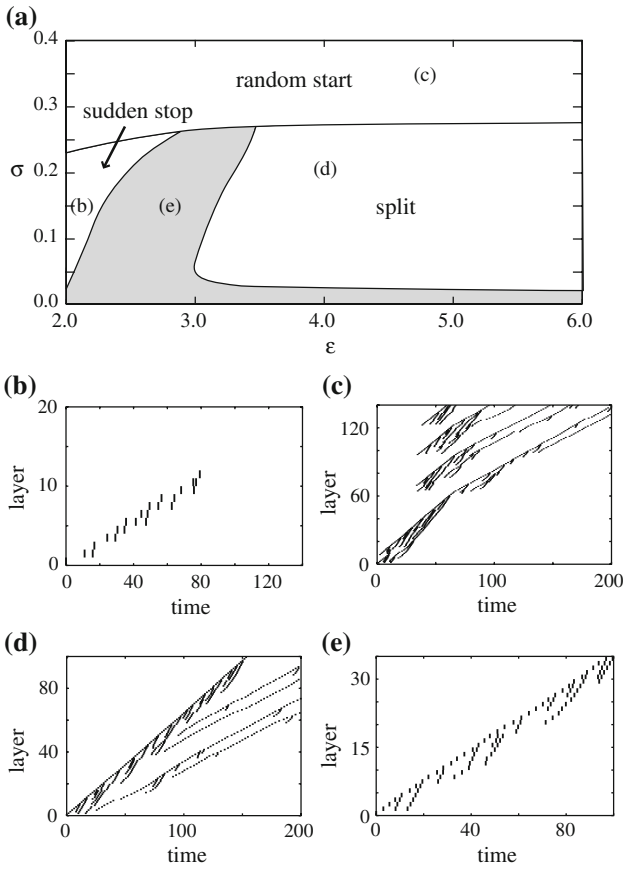

Fig. 8 Phase diagram and raster plots of burst propagation through a chain of single neurons in the presence of background noise. **a** Gaussian white noise of mean zero and variance σ was added to the dynamics of v in Eq. 7. The values of parameters are the same as those in Fig. 1 except that $g_m = 2.8$. *Parenthetic alphabets* indicate the parameter values used below in raster plots. Failed propagation can be classified into three types: sudden stop (**b**), random start (**c**) and split (**d**). **e** Bursts propagate stably with complex evolving temporal profiles in the shaded region of the phase diagram given in (**a**)

5.2 Chains of multi-neuron layers

So far, we have considered propagation of bursts through layers of single neurons, assuming that the size of a unitary excitatory postsynaptic potential (EPSP) is sufficiently large to activate postsynaptic neurons. An actual EPSP, however, is not so large, and coincident inputs from multiple neurons are required to evoke spikes from a postsynaptic neuron. In this subsection, we study how bursts propagate through a chain in the presence of noise when individual layers are comprised of multiple neurons.

Figure 9 displays a phase diagram for a chain of layers of multiple neurons. Each neuron in a layer receives inputs from ten neurons in the previous layer. Accordingly, the weight of each synapse is reduced approximately by a factor of 10, so that the total amplitude of EPSPs remains unchanged from the previous subsection. Compared to Fig. 8, the region of successful burst propagation is much wider in Fig. 9. As in Fig. 8, three types of failure are observed (Fig. 9b, c). Successful propagation can be classified into two subtypes. When the coupling is small, bursts can propagate through layers, preserving an almost fixed temporal profile (Fig. 9d and left panels of Fig. 10). When the coupling is large, burst propagation is accompanied by a complex evolving profile: the times of intraburst spikes change significantly from layer to layer (Fig. 9e and right panels of Fig. 10). The bursting

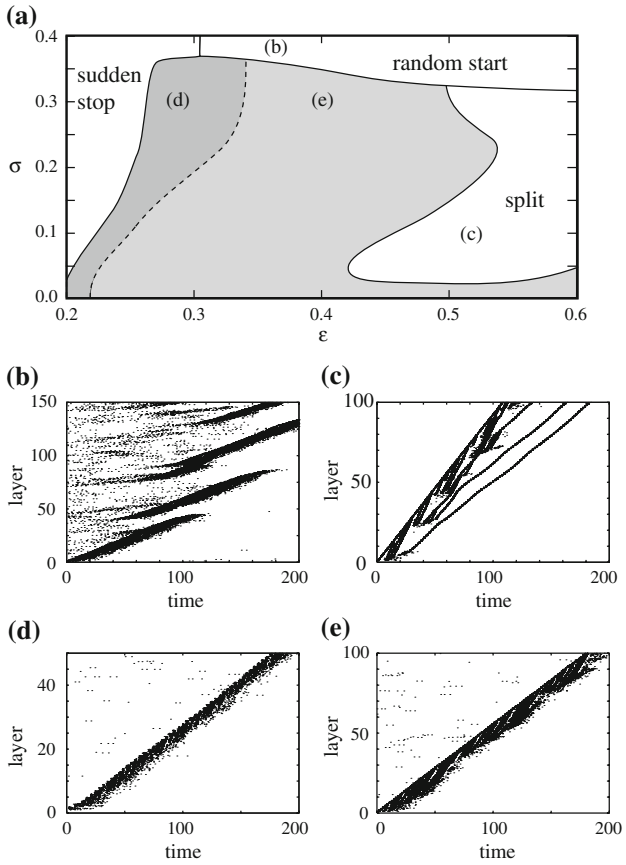

Fig. 9 Phase diagram and raster plots of burst propagation through layers of multiple neurons in the presence of background noise. **a** Each layer consists of 20 neurons that receive inputs from 10 neurons in the previous layer. The values of parameters are the same as in Fig. 8. *Parenthetic alphabets* show the parameters used below in raster plots. As in Fig. 8, failed propagation can be classified into three types (**b**, **c**). Successful propagation is classified into two subtypes: **d** bursts propagate stably keeping almost fixed profiles (corresponding to the *dark shaded region* in (**a**)) or (**e**) they propagate showing complex evolving profiles (corresponding to the light shaded region in (**a**); see also Fig. 10). After a burst passes a layer, sporadic spikes are strongly suppressed in the layer by the hyperpolarization of the membrane potentials

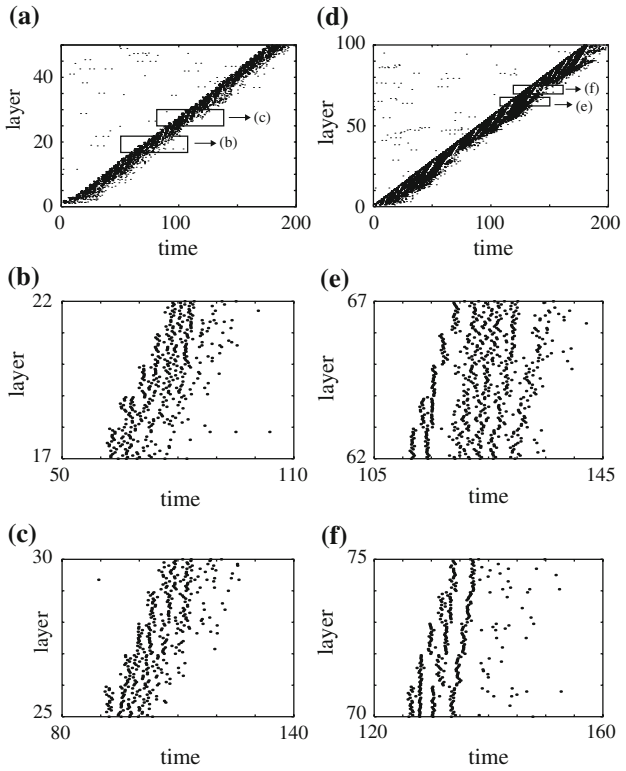

Fig. 10 Propagation through layers of multiple neurons with and without evolving profiles in the presence of background noise. Raster plots in (**a**) and (**d**) are the same as those in Fig. 9d and e, respectively. Raster plots in (**b**) and (**c**) are magnified versions of (**a**), and those in (**e**) and (**f**) are magnified versions of (**d**). Burst propagation alternates between irregular asynchronous firing (**e**) and near-synchronous regular firing (**f**)

pattern is regular and spikes are coincident in some layers (Fig. 10e), while the spike timing is highly diverse in other layers (Fig. 10f). As shown in the previous sections, complex propagation patterns emerge from the intrinsic dynamics of bursting since the strength of noise is identical in all layers.

6 Conclusions and discussion

We have shown that bursts propagate stably through a feed-forward network with a periodic or an irregularly-evolving profile. The timing shifts of intraburst spikes determine the conditions that generate stable burst propagation with or without a fixed temporal profile. Strong couplings between the layers enhance the stability of burst propagation without a fixed profile. The complex evolution of the bursting profile is not impeded by background noise. Noisy input produces differential effects on the bursting patterns in different layers: the times of intraburst spikes are widely scattered by noise in some layers, while a regular temporal arrangement is maintained in other layers. We have used a delta-function-like input from previous layers. We have verified that our model gives essentially the same results for synaptic input with a finite decay constant as long as it is sufficiently smaller than the typical value of ISIs.

Complex spatio-temporal patterns of burst propagation may enrich signal transmissions through feed-forward neuronal networks. It is intriguing to study how various bursting patterns may be utilized in cortical computations, or to evaluate the capacity of heterogeneous feed-forward networks (see, for instance, Teramae and Fukai 2007a) in propagating various bursting patterns. A noise-induced irregular spread of population activities along with their power-law distributions has been reported in a globally coupled system (Teramae and Kuramoto 2001). Analysis of critical population dynamics in unsteady burst propagation will be an interesting future subject.

7 Method

The ionic currents in Eq. 7 are given as $I_{\mathrm{Na}} = g_{\mathrm{Na}} m_{\infty}(v)(v - E_{\mathrm{Na}})$, $I_K(n) = g_K n(v - E_K)$, $I_M(w) = g_M w(v - E_K)$ and $I_{\mathrm{leak}} = g_{\mathrm{leak}}(v - E_{\mathrm{leak}})$, where the steady-state functions are defined as $s_{\infty}(v) = 1/(1 + \exp(-(v_s + v)/h_s))$ for s = m, n and w. Figure 1 was obtained with the following values of parameters: $g_{\mathrm{Na}} = 20.62$, $g_k = 12$, $g_m = 1.5$, $g_{\mathrm{leak}} = 8$, $E_{\mathrm{Na}} = 60$, $E_k = -90$, $E_{\mathrm{leak}} = -80$, $\tau_n = 0.148$, $\tau_w = 100$, $v_m = v_w = 20$, $v_n = 25$, $h_m = 15$, $h_n = h_w = 5$ and $\varepsilon = 1.8$. The units for the conductance, voltage and decay constant are [mS], [mV] and [msec], respectively.

Acknowledgments The authors thank A. D. Reyes, H. Cateau and Y. Tsubo for fruitful discussions and valuable comments. The present work was supported by Grant-in-Aid for Young Scientists (B) 50384722 and Grant-in-Aid for Scientific Research 17022036 from the Japanese Ministry of Education, Culture, Sports, Science and Technology.

References

Abeles M (1991) Corticonics: neuronal circuits of the cerebral cortex. Cambridge University Press, Cambridge

Beggs JM, Plenz D (2004) Neuronal avalanches are diverse and precise activity patterns that are stable for many hours in cortical slice cultures. J Neurosci 24:5216–5229

Belykh I, de Lange E, Hasler M (2005) Synchronization of bursting neurons: what matters in the network topology. Phys Rev Lett 94:188101

Butera RJ, Rinzel J, Smith JC (1999) Model of respiratory rhythm generation in the pre-botzinger complex. I. Bursting pacemaker neurons. J Neurophysiol 82:382–397

Cateau H, Fukai T (2001) Fokker–Planck approach to the pulse packet propagation in synfire chain. Neural Netw 14:675–685

Chaté H, Manneville P (1987) Transition to turbulence via spatio-temporal intermittency. Phys Rev Lett 58:112–115

Chay TR, Keizer J (1983) Minimal model for membrane oscillations in the pancreatic β-cell. Biophys J 42:181–190

Destexhe A, Contreras D (2006) Neuronal computations with stochastic network states. Science 314:85–90

Diesmann M, Gewaltig M, Aertsen A (1999) Stable propagation of synchronous spiking in cortical neural networks. Nature 402:529–533

Elezgaray J, Arneodo A (1992) Crisis-induced intermittent bursting in reaction-diffusion chemical systems. Phys Rev Lett 68:714–717

Fellous JM, Tiesinga PH, Thomas PJ, Sejnowski TJ (2004) Discovering spike patterns in neuronal responses. J Neurosci 24:2989–3001

Gammaitoni L, Hänggi P, Jung P, Marchesoni F (1998) Stochastic resonance. Rev Mod Phys 70:223–287

Galan RF, Ermentrout GB, Urban NN (2005) Efficient estimation of phase-resetting curves in real neurons and its significance for neural-network modeling. Phys Rev Lett 94:158101

Guckenheimer J, Holmes P (1983) Nonlinear oscillations, dynamical systems, and bifurcations of vector fields. Springer, New York

Hahnloser RH, Kozhevvnikov AA, Fee MS (2002) An ultra-sparse code underlies the generation of neural sequences in a songbird. Nature 419:65–70

Han SK, Kurrer C, Kuramoto Y (1995) Dephasing and bursting in coupled neural oscillators. Phys Rev Lett 75:3190–3193

Hansel D, Mato G, Meunier C (1995) Synchrony in excitatory neural networks. Neural Comput 7:307–337

Hindmarsh JL, Rose RM (1984) A model of neuronal bursting using three coupled first order differential equations. Proc R Sci Lond B 221:87–102

Ivanchenko MV, Osipov GV, Shalfeev VD, Kurths J (2004) Phase synchronization in ensembles of bursting oscillators. Phys Rev Lett 93:134101

Izhikevich EM (2000) Neural excitability, spiking and bursting. Int J Bifurcation Chaos 10:1171–1266

Izhikevich EM (2006) Dynamical systems in neuroscience: the geometry of excitability and bursting. MIT, Cambridge

Jin DZ, Ramazanoglu FM, Seung HS (2007) Intrinsic bursting enhances the robustness of a neural network model of sequence generation by avian brain area HVC. J Comput Neurosci 23(3):283–299

Kuramoto Y (1984) Chemical oscillations, waves and turbulence. Springer, Berlin

MacLean JN, Watson BO, Aaron GB, Yuste R (2005) Internal dynamics determine the cortical response to thalamic stimulation. Neuron 48:811–823

Medvedev GS (2006) Transition to bursting via deterministic chaos. Phys Rev Lett 97:048102

Mehring C, Hehl U, Kubo M, Diesmann M (2003) Aertsen A Activity dynamics and propagation of synchronous spiking in locally connected random networks. Biol Cybern 88:395–408

Meucci R, Di Garbo A, Allaria E, Arecchi FT (2002) Autonomous bursting in a homoclinic system. Phys Rev Lett 88:144101

Netoff TI, Banks MI, Dorval AD, Acker CD, Haas JS, Kopell N, White JA (2005) J Neurophysiol 93:1197–1208

Nowotny T, Rabinovich M (2007) Dynamical origin of independent spiking and bursting activity in neural microcircuits. Phys Rev Lett 98:128106

Osipov GV, Ivanchenko MV, Kurths J, Hu B (2005) Synchronized chaotic intermittent and spiking behavior in coupled map chains. Phys Rev E 71:056209

Prut Y, Vaadia E, Bergman H, Haalman I, Slovin H, Abeles M (1998) Spatiotemporal structure of cortical activity: properties and behavioral relevance. J Neurophysiol 79:2857–2874

Raghavachari S, Glazier JA (1999) Waves in diffusively coupled bursting cells. Phys Rev Lett 82:2991–2994

Reyes AD, Fetz EE (1993) Two modes of interspike interval shortening by brief transient depolarizations in cat neocortical neurons. J Neurophysiol 69:1661–1672

Rinzel J, Troy WC (1982) Bursting phenomena in a simplified Oregonator flow system model. J Chem Phys 76(4):1775–1789

Rinzel J (1987) A formal classification of bursting mechanisms in excitable systems. In: Teramoto E, Yamaguti M (eds) Mathematical topics in population biology, morphogenesis, and neurosciences. Lect Notes Biomath 71:267–281

Rulkov NF (2001) Regularization of synchronized chaotic bursts. Phys Rev Lett 86:183–186

Shilnikov A, Cymbalyuk G (2005) Transition between tonic spiking and bursting in a neuron model via the blue-sky catastrophe. Phys Rev Lett 94:048101

Takekawa T, Aoyagi T, Fukai T (2007) Synchronous and asynchronous bursting states: role of intrinsic neural dynamics. J Comput Neurosci 23(2):189–200

Teramae J, Fukai T (2007a) Local cortical circuit model inferred from power-law distributed neuronal avalanches. J Comput Neurosci 22(3):301–312

Teramae J, Fukai T (2007b) Sequential associative memory with nonuniformity of the layer sizes. Phys Rev E 75:011910

Teramae J, Kuramoto Y (2001) Strong desynchronizing effects of weak noise in globally coupled systems. Phys Rev E 63:036210

Teramae J, Tanaka D (2004) Robustness of the noise-induced phase synchronization in a general class of limit cycle oscillators. Phys Rev Lett 93:204103

Teramae J, Tanaka D (2006) Noise induced phase synchronization of a general class of limit cycle oscillators. Prog Theol Phys Supple 161:360–363

Terman D (1991) Chaotic spikes arising from a model of bursting in excitable membranes. SIAM J Appl Math 51:1418–1450

Tsubo Y, Takada M, Reyes AD, Fukai T (2007a) Layer and frequency dependencies of phase response properties of pyramidal neurons in rat motor cortex. Eur J Neurosci 25:3429–3441

Tsubo Y, Teramae J, Fukai T (2007b) Synchronization of excitatory neurons with strongly heterogeneous phase responses. Phys Rev Lett 99:228101

Van Rossum MC, Turrigiano GG, Nelson SB (2002) Fast propagation of firing rates through layered networks of noisy neurons. J Neurosci 22:1956–1966

Vries GC, Sherman A (2000) Channel Sharing in Pancreatic β-cells revisited: enhancement of emergent bursting by noise. J Theor Biol 207:513–530

Wang XJ (1993) Genesis of bursting oscillations in the Hindmarsh-Rose model and homoclinicity to a chaotic saddle. Physica D 62:263–274

Zhou C, Kurths J (2002) Noise-induced phase synchronization and synchronization transitions in chaotic oscillators. Phys Rev Lett 88:230602